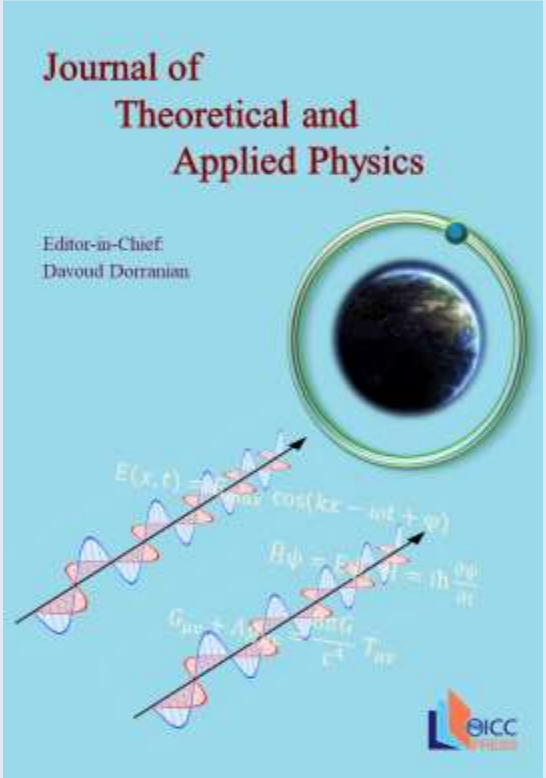

ACCEPTED PAPER

Bohm sheath criterion for electronegative warm plasma carrying seconadary electron emission in an oblique magnetic field

Yetendra Prasad Jha[1], Mayank Kumar[2], Hitendra K. Malik[*1]

[1]*Plasma Science and Technology Laboratory, Department of Physics, Indian Institute of Technology Delhi, New Delhi, India*
[2]*Department of Mechanical Engineering, Indian Institute of Technology Delhi, New Delhi, India*

hkmalik@physics.iitd.ac.in

Received: 23 October 2022;

Accepted: 10 January 2023;

http://dx.doi.org/10.57647/J.JTAP.2023.1702.32

Oxford OX29 4DA; GB; https://oiccpress.com;

Bohm sheath criterion for electronegative warm plasma carrying seconadary electron emission in an oblique magnetic field

Yetendra Prasad Jha[1], Mayank Kumar[2], Hitendra K. Malik*[1]

[1]*Plasma Science and Technology Laboratory, Department of Physics, Indian Institute of Technology Delhi, New Delhi-110016, INDIA*
[2]*Department of Mechanical Engineering, Indian Institute of Technology Delhi, New Delhi-110016, INDIA*

*Corresponding author: hkmalik@physics.iitd.ac.in**

Abstract

The Bohm sheath criterion is formulated by using Sagdeev potential approach for electronegative warm plasma under oblique magnetic field and secondary electron emission from the wall. In this model the effect of collisions between positive ions and neutral, ionization, electronegativity, non-extensivity and temperature ratio (positive/negative ion to electron) are also considered to get the exact behavior of velocity of positive ions at the edge of the sheath. Results are compared with the cases of collision-less, ionization-less and absence of electron emission from the wall and it is found that the Bohm velocity for this case is decreased faster with the increase of non-extensivity and the angle of inclination of the applied magnetic field. Also, Bohm velocity gets increased when the electric field at the edge of the sheath increases. Although Bohm velocity does not depend on the strength of the magnetic field, but the slope in the electrostatic potential gets increased and the sheath thickness decreased on raising the strength of the magnetic field.

1. Introduction

The sheath formation takes place when an absorbing or conducting wall is in contact with plasma. The sheath plays an important role in plasma wall interaction (PWI). In current years a lot of attention has been given to sheath formation mechanism due to its application to plasma processing technology [1,2], thin film deposition [3-6], magnetic confinement fusion plasma and lab plasma. To improve the lifetime and performance of electric propulsion (EP) devices [7,8] the effect of sheath has been studied by the researchers. If the unwanted effects of PWI are mitigated then it can improve the thruster parameters such as total thruster efficiency, thrust density and propellent ionization efficiency [9]. In a simplified model it has been observed that the electrons, having a higher mobility than the ions, when bombard the wall can create a negative potential on the wall with respect to the plasma. Now to balance the flow of ions and electrons to the wall there is the formation of positive space charge adjacent to the wall (region known as sheath) while adjacent to the plasma there is the region of presheath which functions to full fill the well-known Bohm criterion. The width of the sheath is in a few Debye radius while of the presheath is determined by the size of plasma container or by the ion mean free path. These two regions have different characteristics and functions, and hence the plasma boundary problem is solved in two scales separately. The electric field is considered zero in the presheath on the sheath scale considering the presheath region as infinitely large. So, an appropriate boundary condition is required for modelling the sheath because it affects both the sheath as well as the bulk plasma. For example, in tokamak the sheath boundary condition is involved in plasma edge transport process phenomenon [10,11]. In the absence of magnetic field, the minimum required velocity of ions, i.e., the Bohm velocity, for a weakly collisional plasma has been given by the researchers [12-14] as

$$u_{iz} \geq C_s = \sqrt{\frac{k_B(T_e + \gamma T_i)}{M_i}}$$

Here C_s is the ion acoustic speed, k_B is the Boltzmann constant, T_e is the electron temperature, T_i is the ion temperature and M_i is the mass of ions. $\gamma = 1$ is taken in the case of isothermal approximation, otherwise $\gamma = 3$, 2 and $\frac{5}{3}$ for one-, two- and three-dimensional adiabatic approximations, respectively. In presence of an oblique magnetic field, it has been shown numerically by the researchers that the ion velocity at the sheath edge should be greater than the ion acoustic speed and it also depends on the incident angle θ of the magnetic field [15,16] for a weakly collisional plasma sheath. Specifically, the relation between the ion velocity u_{iz} and the ion acoustic speed C_s reads

$$u_{iz} = C_s \cos\theta.$$

Generally, the effects of ionization and collisions can be neglected in weakly collisional sheath while in strong collisional sheath the ionization and collisions affect the sheath structure as well as the Bohm criterion. Few researchers [17-19] have considered the collisional plasma sheath attempting to see the effects of magnetic field and collisions in their model. They have found that the collisions diminish the influence of magnetic field on the velocity of ions at the sheath edge in a cold ion plasma. But in the magnetic confinement fusion plasma, the edge tokamak plasma contains the ions having temperature comparable to that of the electrons, sometimes the temperature of the positive ions is even higher than that of the electrons. Few researchers [20,21] have considered the effect of the ion temperature along with the collisions and external magnetic field on Bohm criterion and have shown that the temperature of ions affects the properties of sheath.

During the plasma-wall interaction, the emission of electrons takes place from the wall due to the bombardment of electrons and ions on the wall. The electrons having energy greater than 30 eV and the ions having energies greater than 10 keV can produce secondary electron emission from the wall [22-26]. In fusion plasmas [27-30], the wall gets heated due to the plasma itself that is present in the container, because of which the thermionic emission of electrons may occur. Here the sheath between the plasma and the wall acts as an insulator, trying to isolate the wall from the particles and heat transfer. But the electron emission influences the sheath characteristics, and it reduces the electrostatic potential inside the sheath which increases the heat flux and particle flux to the wall. Ultimately the plasma surface treatment sputtering process, ion implantation and particle/energy transport get influenced by these emitted electrons from the wall. The sheath with emitted electrons has been theoretically investigated by the researchers [31-39] considering the Boltzmann distribution of the electrons. But it is generally experienced that there exist systems where there is a deviation from this Boltzmann distribution [40,41]. These types of the systems are known as non-extensive and have been explained by Tsallis [42]. On the other hand, the behavior of sheath has also been found to be influenced by the introduction of negative ions [43,44]. In the present article, we consider a plasma system having the positive ions of finite temperature, negative ions, collisions, ionization, and electrons with non-extensive distribution under the effect of external magnetic field. With the inclusion of all these parameters in the model, Bohm sheath criterion is obtained analytically by applying Sagdeev potential approach. Largely the electrostatic potential is plotted for various parameters to show the general picture of plasma-wall interaction.

2. Theoretical Model

In our model, the positive ions and secondary electrons are described by the fluid equations, i.e., continuity and momentum transfer equations. The bulk plasma electrons are described by the non-extensive distribution while the negative ions are in thermodynamic equilibrium following the Boltzmann distribution. The magnetic field is applied obliquely to the wall in the x-z plane, while the electric field is in the z-direction (as shown in Fig. 1). Under the said arrangement, the $\mathbf{E} \times \mathbf{B}$ drift is only in the y-direction. We have assumed that the wall is infinitely long in the x- & y-directions, which means that the sheath is homogenous in x-y plane and the physical properties change only in the z-direction, i.e., normal to the wall. The edge of the sheath is taken to be at $z = 0$.

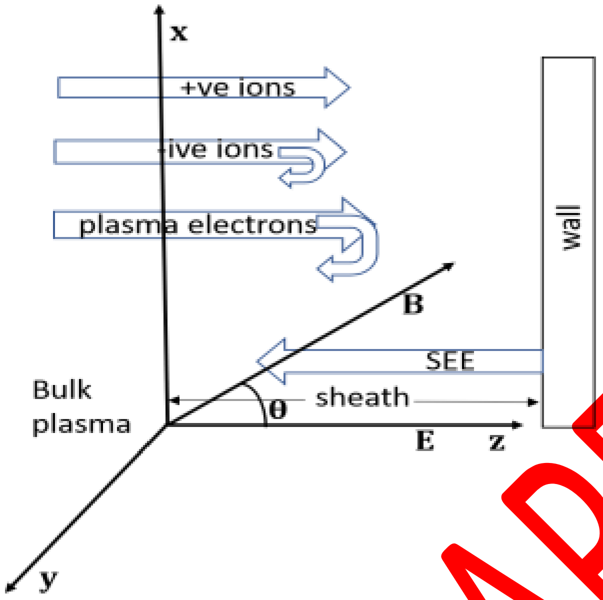

Figure 1. Schematic diagram depicting the magnetic configuration and secondary electron emission from the wall.

The expression of the magnetic field **B** and the basic equations for the positive ions under the said situation read

$$\mathbf{B} = B_0\cos\theta\hat{z} + B_0\sin\theta\hat{x} \tag{1}$$

$$\frac{d}{dz}\left(n_p v_{pz}\right) = \nu_{iz} n_e \tag{2}$$

$$M_p n_p v_{pz}\frac{dv_{px}}{dz} = en_p v_{py} B_0\cos\theta - M_p n_p \nu v_{px} - M_p n_e \nu_{iz} v_{px} \tag{3}$$

$$M_p n_p v_{pz}\frac{dv_{py}}{dz} = en_p\left(v_{pz}B_0\sin\theta - v_{px}B_0\cos\theta\right) - M_p n_p \nu v_{py} - M_p n_e \nu_{iz} v_{py} \tag{4}$$

$$M_p n_p v_{pz}\frac{dv_{pz}}{dz} = en_p\left(-\frac{d\eta}{dz} - v_{py}B_0\sin\theta\right) - k_B T_p\frac{dn_p}{dz} - M_p n_p \nu v_{pz} - M_p n_e \nu_{iz} v_{pz} \tag{5}$$

In the above equations, n_p and n_e are the density of positive ions and electrons, respectively. v_{px}, v_{py} and v_{pz} are the velocity components of the positive ions along x-, y- and z-directions, respectively. ν_{iz} is the ionization frequency. ν is the collision frequency. B_0 is the magnetic field strength. M_p and T_p are respectively the mass and temperature of the positive ions. η is the potential inside the sheath with respect to the edge.

The density distribution of the bulk plasma electrons is given by

$$n_e = n_{e0}\left(1 + (q-1)\frac{e\eta}{k_B T_e}\right)^{\frac{(3q-1)}{(2q-2)}} \tag{6}$$

Here q is the non- extensivity parameter. n_{e0} and T_e are respectively the background density and temperature of the electrons. e is the electronic charge.

The density distribution of the negative ions is given by

$$n_n = n_{n0}\exp\left(-\frac{e\eta}{k_B T_n}\right) \tag{7}$$

Here n_{n0} is the background density of the negative ions and T_n is their temperature.

The secondary electrons are governed by the following equations

$$\frac{d}{dz}(n_s v_{sz}) = 0 \tag{8}$$

$$m_s v_{sz} n_s \frac{dv_{sx}}{dz} = -eB_0\, v_{sy}\sin\theta \tag{9}$$

$$m_s v_{sz} n_s \frac{dv_{sy}}{dz} = eB_0(v_{sx}\cos\theta - v_{sz}\sin\theta) \tag{10}$$

$$m_s v_{sz} n_s \frac{dv_{sz}}{dz} = eB_0\left(-\frac{d\eta}{dz} - k_B T_s\frac{dn_s}{dz} + v_{sy}\sin\theta\right) \tag{11}$$

Here n_s is the density of the secondary electrons and v_{sx}, v_{sy} and v_{sz} are respectively their velocity components along x-, y- and z-directions.

The densities are normalized by the background density of the electrons n_{e0}, velocity components are normalized by $C_{sp} = \sqrt{\frac{k_B T_e}{M_p}}$, the distance is normalized by the Debye length $\lambda_{de} = \sqrt{\frac{\varepsilon_0 k_B T_e}{n_{e0} e^2}}$ and the potential is normalized by $\frac{k_B T_e}{e}$. Hence, the quantities in terms of the normalized parameters are written below.

$u_p = \frac{v_p}{C_{sp}}$; $u_n = \frac{v_n}{C_{sp}}$; $\xi = \frac{z}{\lambda_{de}}$; $\phi = -\frac{e\eta}{k_B T_e}$; $\lambda = \frac{v}{v_{iz}}$; $\gamma_p = \frac{T_p}{T_e}$; $\gamma_n = \frac{T_n}{T_e}$; $t_s = \frac{T_s}{T_e}$ $N_e = \frac{n_e}{n_{e0}}$; $N_P = \frac{n_P}{n_{e0}}$; $N_N = \frac{n_N}{n_{e0}}$; $N_S = \frac{n_S}{n_{e0}}$; $\omega_{pi} = \sqrt{\frac{n_{e0} e^2}{\varepsilon_0 M_p}}$; $\omega_{ic} = \frac{eB}{M_p}$; $\beta = \frac{\omega_{ic}}{\omega_{pi}}$; $r = \frac{\lambda_{de}}{\Lambda}$; $\Lambda = \frac{C_{sp}}{v_{iz}}$.

Here N_p is the normalized density of the positive ions, and u_{px}, u_{py} and u_{pz} are their normalized velocity components, λ is the collisional parameter, r is the non-neutrality parameter for ionization and β is the ratio of ion cyclotron frequency to the ion plasma frequency. ε_0 is the permittivity of free space, Λ is the ionization length, N_e and N_n are the normalized densities of the electrons and negative ions, respectively, N_{e0} and N_{n0} are the normalized densities of the positive and negative ions, respectively at the sheath edge, N_s is the normalized density of secondary electrons, and u_{sx}, u_{sy} and u_{sz} are their normalized velocity components. γ_p, γ_n and t_s are the temperature ratios.

The basic equations in the normalized form are written below

$$\frac{d}{d\xi}(N_p u_{pz}) = rN_e \tag{12}$$

$$\frac{du_{px}}{d\xi} = \frac{1}{u_{pz}}\left(u_{py}\beta\cos\theta - \lambda u_{px} r - \frac{N_e}{N_p}u_{px} r\right) \tag{13}$$

$$\frac{du_{py}}{d\xi} = \frac{1}{u_{pz}}\left(\beta\sin\theta - u_{px}\beta\cos\theta - \lambda u_{py} r - \frac{N_e}{N_p}u_{py} r\right) \tag{14}$$

$$\frac{du_{pz}}{d\xi} = \left(1 - \frac{\gamma_p}{u_{pz}^2}\right)^{-1}\left(\frac{1}{u_{pz}}\frac{d\phi}{dz} - \frac{\beta u_{py}\sin\theta}{u_{pz}} - \gamma_p r\frac{N_e}{N_p}\frac{1}{u_{pz}^2} - \lambda r - \frac{N_e}{N_p} r\right) \tag{15}$$

$$N_e = (1-(q-1)\phi)^{\frac{(3q-1)}{(2q-2)}} \tag{16}$$

$$N_n = N_{n0}\exp\left(-\frac{\phi}{\gamma_n}\right) \tag{17}$$

$$\frac{d}{d\xi}(N_s u_{sz}) = 0 \tag{18}$$

$$\frac{du_{sx}}{d\xi} = -\beta\frac{u_{sy}}{u_{sz}}\sin\theta \tag{19}$$

$$\frac{du_{sy}}{d\xi} = \frac{\beta}{u_{sz}}(u_{sx}\cos\theta - u_{sz}\sin\theta) \tag{20}$$

$$\frac{du_{sz}}{d\xi} = \frac{\mu_s}{u_{sz}}\left(-\frac{d\phi}{d\xi} - \frac{t_s}{N_s}\frac{dN_s}{dz} + \beta u_{sy}\sin\theta\right) \tag{21}$$

Poisson's equation in the normalized form is written as

$$\frac{d^2\phi}{d\xi^2} = (N_p - N_n - N_e - N_s) \tag{22}$$

Finally, the neutrality condition in the normalized form reads

$$N_{p0} \cong 1 + N_{n0} + N_{s0} \tag{23}$$

The solution of second order differential equation (22) can be found by using numerical methods [38,45-48]. Generally for solving this type of coupled differential equations we use Runge- Kutta (ODE-45) where boundary conditions are also applied. To get the Bohm velocity by using Sagdeev's potential approach we multiply the Poisson's equation (22) by ϕ' (prime refers to the derivate) and then integrate it to get

$$\frac{\phi'^2}{2} - \frac{\phi'^2_0}{2} = -\psi_S(\phi, u_{p0z}) \tag{24}$$

where $\psi_S(\phi, u_{p0z}) = -\int_0^{\phi}(N_p - N_n - N_e - N_s)d\phi$ is the Sagdeev potential. At the sheath edge

$$\psi_S(0, u_{p0z}) = 0 \text{ and } \frac{\partial}{\partial\phi}\psi_S(0, u_{p0z}) = 0 \quad .$$

$\frac{\partial^2}{\partial\phi}\psi_S(0, u_{p0z}) < 0$ is the maximising condition for the Sagdeev potential. Following this method, the z-component of the velocity of the positive ions at the edge of sheath i.e., Bohm velocity is calculated, where the relation of the y-component of the positive ion velocity and the secondary emitted electrons $u_{p0y} = \frac{\phi'_0 \sin\theta}{\beta} = u_{s0y}$ is used. Hence, the ion velocity at the edge is given by

$$u_{p0z} = \frac{\left(\frac{-2r+\lambda r N_{p0}}{\phi'_0}\right) + \sqrt{\left(\frac{-2r+\lambda r N_{p0}}{\phi'_0}\right)^2 + 4\left(\frac{N_{n0}}{\gamma_n} + \frac{(3q-1)}{2} - \frac{\mu_s N_{s0}\cos^2\theta}{(u_{sx0}^2 - \mu_s t_s)}\right)\left(N_{p0}\cos^2\theta + \frac{N_{n0}}{\gamma_n}\gamma_p + \frac{(3q-1)}{2}\gamma_p\right)}}{2\left(\frac{N_{n0}}{\gamma_n} + \frac{(3q-1)}{2} - \frac{\mu_s N_{s0}\cos^2\theta}{(u_{sx0}^2 - \mu_s t_s)}\right)} \tag{25}$$

2.1 Limiting cases

(a) For the normal incidence of the magnetic field, we have $\theta = 0^0$ and $\cos\theta \rightarrow 1$ and the above expression reduces to

$$u_{p0z} = \frac{\left(\frac{-2r + \lambda r N_{p0}}{\phi'_0}\right) + \sqrt{\left(\frac{-2r + \lambda r N_{p0}}{\phi'_0}\right)^2 + 4\left(\frac{N_{n0}}{\gamma_n} + \frac{(3q-1)}{2} - \frac{\mu_s N_{s0}}{(u_{sx0}^2 - \mu_s t_s)}\right)\left(N_{p0} + \frac{N_{n0}}{\gamma_n}\gamma_p + \frac{(3q-1)}{2}\gamma_p\right)}}{2\left(\frac{N_{n0}}{\gamma_n} + \frac{(3q-1)}{2} - \frac{\mu_s N_{s0}}{(u_{sx0}^2 - \mu_s t_s)}\right)}$$

(b) For collision-less and ionization free electropositive plasma without electron emission, we have $\lambda = 0$, $r = 0$, $N_{n0} = 0$ and $N_{s0} = 0$. Then the relation reads

$$u_{p0z} \geq \sqrt{\frac{2}{(3q-1)}}\cos\theta$$

This result matches with the expression obtained by Safa et al. [49].

(c) For collision-less and ionization free electronegative warm plasma without electron emission, $\lambda = 0$, $r = 0$, and $N_{s0} = 0$. Then the relation reads

$$u_{p0z} \geq \sqrt{\gamma_p + \frac{2N_{p0}\cos^2\theta}{\left(\frac{2N_{n0}}{\gamma_n} + (3q-1)\right)}}$$

This is the same expression as obtained by Asserghine et al. [50].

(d) For collision-less, ionization free, un-magnetized, electropositive plasma with cold ions, Boltzmann distributed electrons and without emission of electrons from the wall we have $\lambda = 0$, $r = 0$, $\gamma_p = 0$, $\beta = 0$, $N_{n0} = 0$, $q \rightarrow 0$ and $N_{s0} = 0$. Under this limiting case, the expression reads

$$u_{p0z} \geq 1$$

This result is the same as given by Chen [51].

3. Results and Discussion

The effect of the electric field ϕ'_0 and inclination angle θ (in degrees) of magnetic field at the sheath edge on the z-component of velocity u_{poz} is plotted in Fig. 2. It is found that as θ increases there is a reduction in the velocity u_{poz}, means the minimum velocity required by the positive ions to enter the sheath gets reduced. The reason behind this is that the increase of the inclination angle makes the Lorentz force stronger on the positive ions in the z-direction, leading to smaller velocity the ions. On the other hand, the value of u_{poz} increases with the increasing field ϕ'_0. Clearly it can be understood that increase in the electric field at the edge of the sheath means there is more electric field in the pre-sheath region and this electric field is responsible for enhancing the velocity of positive ions. This result of dependency of u_{poz} on the angle of inclination also matches with the result of [18].

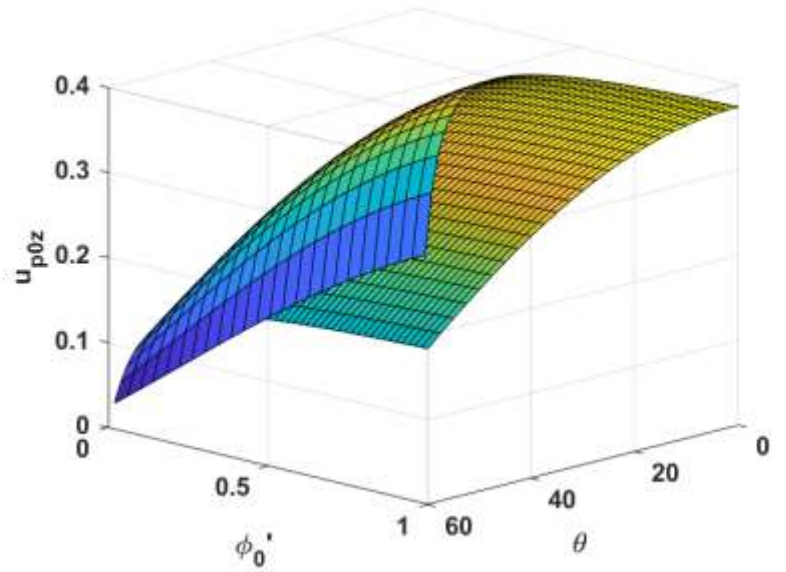

Figure 2. Bohm velocity u_{poz} as a function of magnetic field inclination angle θ (in degrees) and electric field ϕ'_0 at the sheath edge for $N_{n0} = 2$, $N_{s0} = 0.008$, $u_{s0} = 1500$, $\mu_s = 1864$, $t_s = 0.05$, r=0.1, $\gamma_P = 0.1$, $\gamma_n = 0.1$, q=0.5 and $\lambda = 1$.

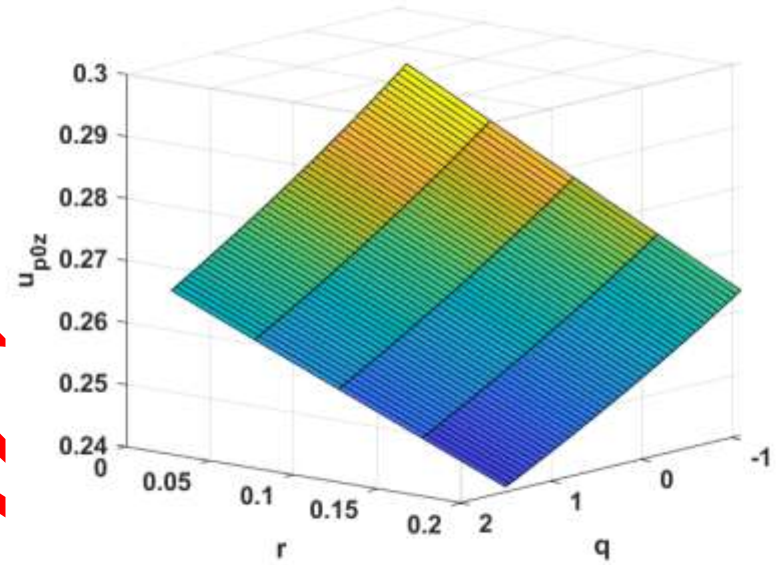

Figure 3. Bohm velocity u_{poz} as a function of ionization parameter *r* and non-extensivity *q* for $N_{n0} = 1$, $N_{s0} = 0.008$, $u_{s0} = 1500$, $t_s = 0.1$, $\mu_s = 1864$, $\theta = 30^0$, $\phi'_0 = 0.8$, r = 0.1, $\gamma_P = 0.001$, $\gamma_n = 0.05$ and $\lambda = 1$.

The non-extensivity and the ionization present inside the plasma play a vital role in the modification of the Bohm velocity which is evident from Fig. 3; here u_{poz} gets decreased with the increasing values of the non-extensivity q. This result matches with the observation of other researchers [52] where they have considered cold positive ions but, in our case, the velocity is decreased mildly. For increase in the non-neutrality parameter *r*, i.e., when ionization increases, the values of u_{poz} get decreased, which may be due to the loss of energy by the ions in the presence of higher ionization in the plasma.

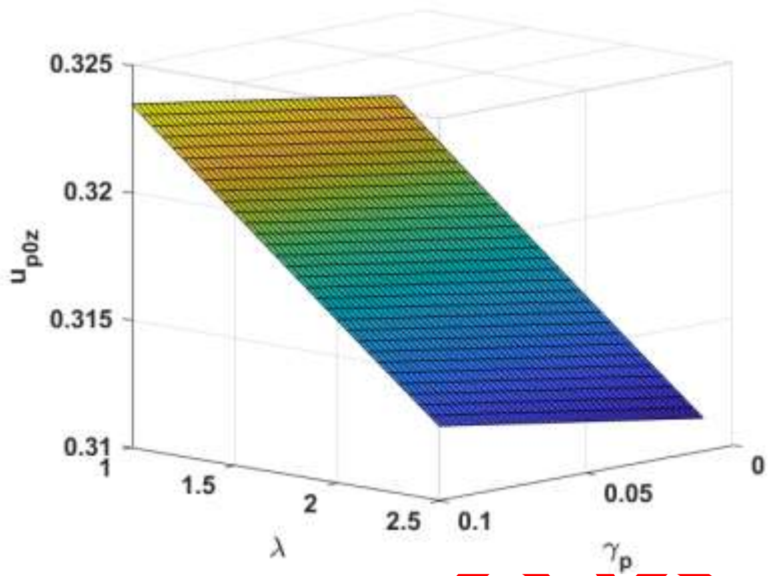

Figure 4. Bohm velocity u_{poz} as a function of positive ion to electron temperature ratio γ_P and collisional parameter λ for $N_{n0} = 2$, $N_{s0} = 0.008$, $u_{s0} = 1500$, $t_s = 0.1$, $\mu_s = 1864$, $\theta = 30^0$, $\phi'_0 = 0.1$, r = 0.1, $\gamma_n = 0.1$ and q = 0.5.

The collisions between the positive ions and neutral atoms affect the minimum velocity required to enter the sheath, i.e., the velocity u_{poz} (Fig. 4). As the collisions are increased, the values of u_{poz} decrease. This is because during the increase in the collision there is more momentum transfer and loss of energy. While increase in the positive ion to electron temperature ratio γ_P results in the insignificant increase in u_{poz}. But researchers have found that with the increase in the temperature of positive ions the Bohm velocity should also increase. This difference in the result is made by the ionization and secondary electron emission from the wall.

The electronegativity N_{n0} is found to have a significant role on the Bohm criterion. This is observed that the negative ions try to help the positive ions to enter the sheath. The velocity u_{poz} gets reduced when the value of N_{n0} is increased. While the increase in the temperature ratio of negative ion increases u_{poz} (Fig. 5). The inclination angle of magnetic field 0^0 and 30^0 are also compared and it can be seen that u_{poz} is more for 0^0(yellow region) than that of 30^0(brown region). This is because the Lorentz force is stronger on the positive ions in the z-direction for 0^0 which reduces with the increase of the inclination angle and hence, the velocity gets reduced though the variation with electronegativity N_{n0} and temperature ratio of negative ion remains the same.

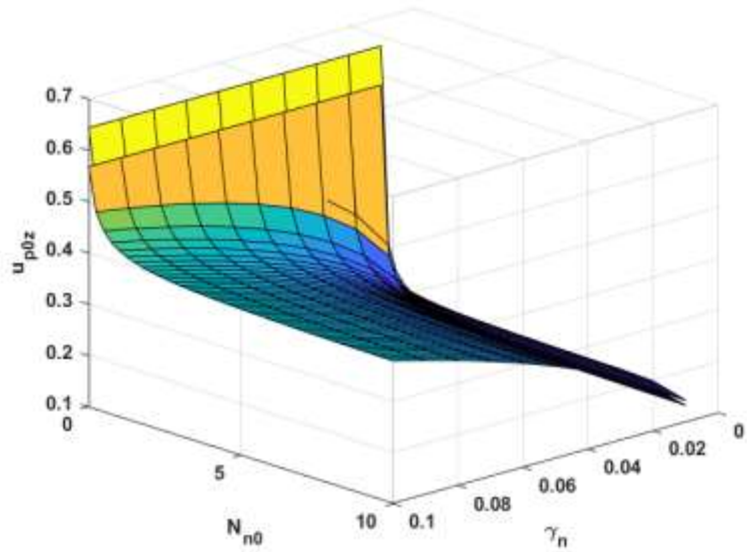

Figure 5. Bohm velocity u_{poz} as a function of electronegativity N_{n0} and negative ion to electron temperature ratio γ_n for $N_{s0} = 0.008$, $u_{s0} = 1500$, $t_s = 0.1$, $\mu_s = 1864$, $\phi'_0 = 0.1$, r = 0.1, $\gamma_p = 0.1$, $q = 0.5$, $\lambda = 1$, $\theta = 0^0$(yellow region) and $\theta = 30^0$(brown region).

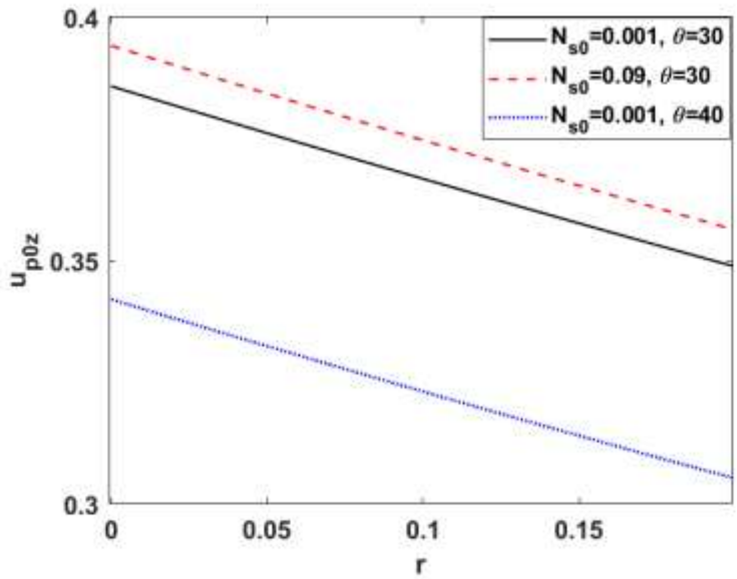

Figure 6. Bohm velocity u_{poz} as a function of normalized ionization parameter *r* for different density of the secondary electrons at the edge of sheath (N_{s0}) and magnetic field inclination angle θ (in degrees) for $N_{n0} = 2$, $u_{s0} = 1500$, $t_s = 0.1$, $\mu_s = 1864$, $\phi'_0 = 0.1$, $\gamma_p = 0.1$, $\gamma_n = 0.1$, $q = 0.5$ and $\lambda = 1$.

The Bohm velocity is plotted as a function of the non-neutrality parameter in Fig. 6. The velocity u_{poz} decreases as non-neutrality parameter is increased. As the density of the secondary electrons at the edge of sheath (N_{s0}) is increased from 0.001 to 0.09, the values of u_{poz} get increased (evident from the red dashed line and solid line in the figure). On the other hand, the velocity u_{poz} gets decreased when the magnetic field inclination angle θ is increased.

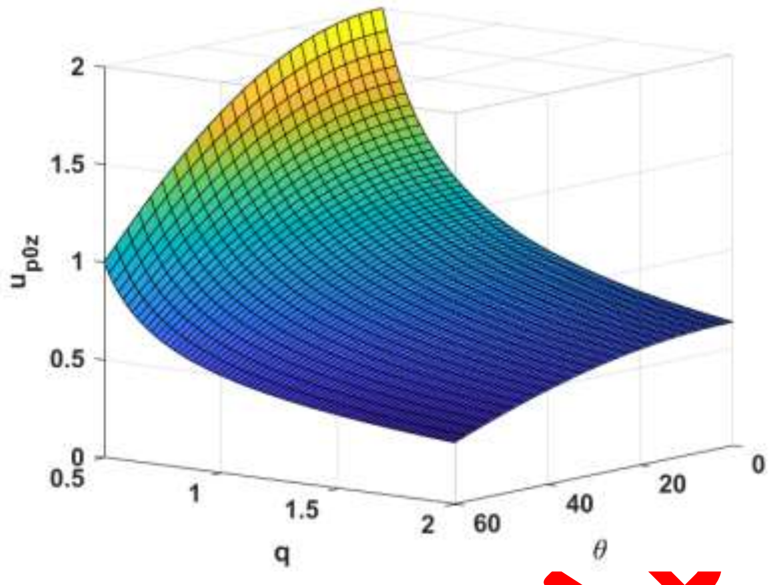

(a)

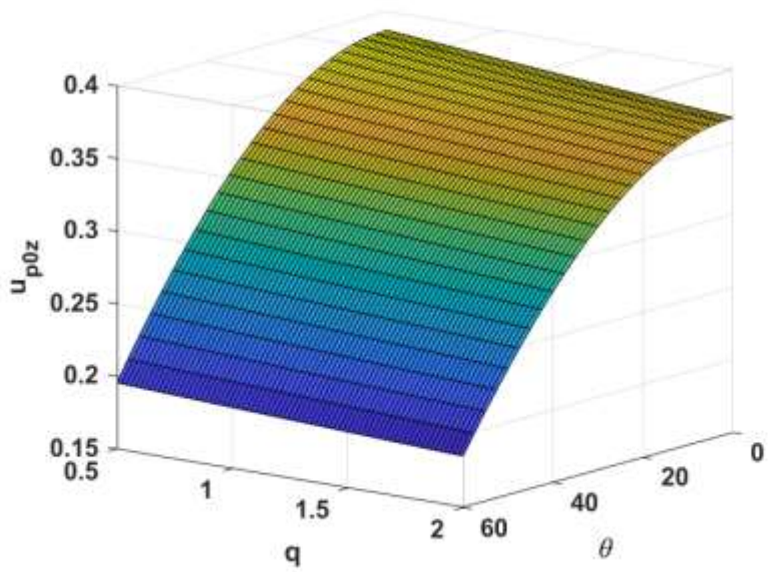

(b)

Figure 7. Bohm velocity u_{poz} as a function of non-extensivity and magnetic field inclination angle θ (in degrees) for (a) collision-less, ionization free, cold ions and zero emission of electrons from the wall (b) collision-less, ionization free, zero emission of electrons from wall in electronegative warm plasma.

When we neglect the collisions, ionization, negative ions / electronegativity, temperature of the positive ions and the electron emission from the wall, then it is found that the decrease in the z-component of the velocity is faster with the increase in the inclination of magnetic field and non-extensivity parameter (Fig. 7a). While this decrease is slower in the presence of the mentioned parameters, as shown in Figs. 2 and 3. However, there is insignificant change in u_{poz} with the increase in q value when the electronegativity and temperature of the positive ions are taken into account. Though u_{poz} decreases with the inclination angle, as shown in Fig. 7b, but not at the rate as it was for the case of Fig. 7a.

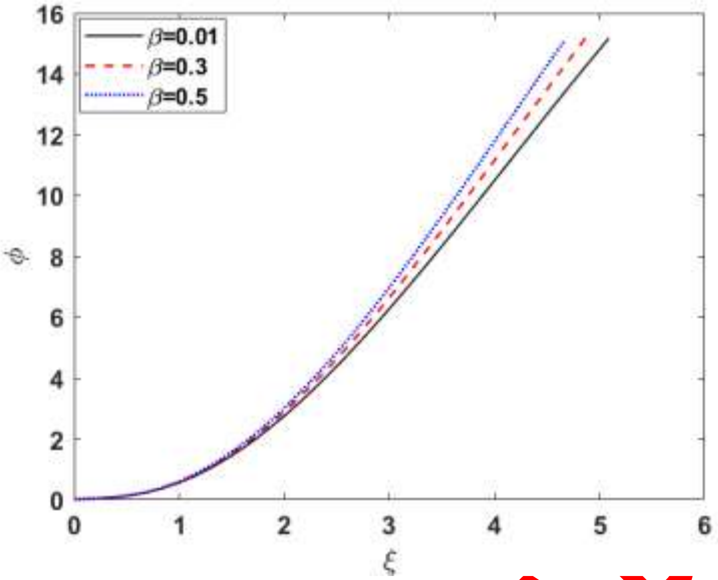

Figure 8. Normalized electrostatic potential as a function of normalized distance for different strength of the magnetic field for $N_{n0} = 2$, $N_{s0} = 2$ $u_{s0} = 100$, $t_s = 0.01$, $\mu_s = 1864$, $\theta = 60^0$, $\phi'_0 = 0.01$, $\gamma_p = 0.1$, $r = 1$, $u_{p0} = 3$, $\gamma_n = 0.1$, $q = 1$ and $\lambda = 1$.

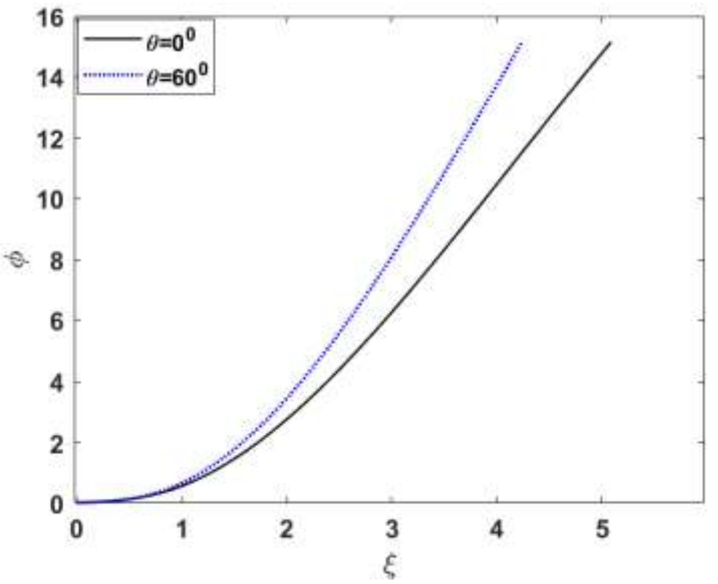

Figure 9. Normalized electrostatic potential as a function of normalized distance for different strength of the magnetic field for $N_{n0} = 2$, $N_{s0} = 0.001$ $u_{s0} = 100$, $t_s = 0.01$, $\mu_s = 1864$, $\phi'_0 = 0.01$, $\gamma_p = 0.1$, $\gamma_n = 0.1$, $r = 0.1$, $u_{p0} = 3$, $q = 0.97$, $\beta = 0.5$, and $\lambda = 1$.

The impact of strength of magnetic field and inclination angle on the electrostatic potential and sheath thickness is shown in Fig. 8 and Fig. 9, respectively. As the magnitude of the magnetic field is increased, though the Bohm velocity is not affected (from equation 25) but the slope of the electrostatic potential gets increased. For example, for the density $n = 10^{16}m^{-3}$, electron temperature $T_e = 2eV$ and the ratio of ion cyclotron frequency to the plasma ion frequency $\beta = 0.01$, the sheath thickness is $5.2 \times 10^{-4}m$. When β is increased to 0.5 the sheath thickness is decreased to $4.5 \times 10^{-4}m$. The magnetic field B is in the units of Tesla. This is due to the reason that on increasing the strength of the magnetic field there is an enhancement in the net space charge density and hence the electrostatic potential also gets increased and the sheath thickness gets reduced. Also, the sheath thickness gets decreased from 5.09×10^{-4}m to 4.24×10^{-4}m when the angle θ is increased from 0^0 to 60^0, as shown in Fig. 9. In the end, this will be worth to mention that our results shall play a crucial and advantageous role in the plasma systems where the magnetic field is externally applied, collisions take place between the positive ions and neutral atoms, non-extensive plasma electrons exist and there is secondary electron emission from the wall. It has been observed through our realistic model that the Bohm velocity at the edge is greatly influenced by the above parameters. To get the desired deposition rate in the magnetron sputtering processes our results will be beneficial where the thin film deposition gets affected by the kinetic energy of the positive ions. Also, in the sputtering systems and ion implantation where the electron emission can take place, our results can give the idea for the optimum parameters needed to achieve good results.

4. Conclusions

The z-component of ion velocity at the sheath edge (Bohm velocity) depends on the collisions, ionization, angle of magnetic field, non-extensivity, temperature ratio (positive / negative ion to electron), electronegativity, density of secondary electrons and electric field at the edge of the sheath. The Bohm velocity is independent of the strength of the applied magnetic field. As the angle of inclination of the magnetic field is increased, the velocity attains lower values. The Bohm velocity increases with the increase in the electric field and density of secondary electrons at the sheath edge and temperature ratio (positive / negative ion to electron). For increase in the collisional parameter, non-neutral parameter (for ionization), extensivity and electronegativity, there is a reduction in the Bohm velocity. On comparing with collision-less, ionization free and no emission of electrons from the wall the Bohm velocity decreases slowly with the increase in the value of non-extensivity and inclination angle of the magnetic field. The electrostatic potential gets affected by the strength of the magnetic field. The sheath thickness reduces on increasing the magnetic field and its obliqueness. Our results find application in the field of plasma processing. These are also applicable to the ion implantation process which is done in the presence of magnetic field. Also, the temperature of ions is included in the model which gives idea about the increase in the ions energy and the longitudinal velocity. In the magnetron sputtering, ion flux to the target can be increased by the variation of the positive ions and hence, the rate of coating can also be increased.

Acknowledgement

The author Yetendra Prasad Jha thanks the UGC-CSIR (Government of India) for supporting this work financially.

References

[1] Dorranian, D., et al.: Structural and optical characterization of PMMA surface treated in low power nitrogen and oxygen RF plasmas. Journal of Non-Oxide Glasses **1** 217-229 (2009).

[2] Jafari, M., & Dorranian, D: Surface modification of PMMA polymer in the interaction with oxygen-argon RF plasma (2011).

[3] Shibata, K., Nishida, Y., & Yugami, N. (1994).: Production of Thin-film by Sheet-shaped Plasma. *Appl. Phys*, **63** 559.

[4] Shibata, K., Ito, H., Yugami, N., Miyazaki, T., & Nishida, Y. Production of Nb thin film by ECR sheet plasma. Thin solid films **386** 291-294 (2001).

[5] Singh, O., et al.: Investigation of titanium nitride thin films treated in hot cathode arc discharge plasma system. Appl. Sci. Lett **2** 37-41 (2016).

[6] Singh, Omveer, et al.: Influence of negative bias voltage on structural and mechanical properties of nanocrystalline TiNx thin films treated in hot cathode arc discharge plasma system. Ceramics International **42** 18019-18024 (2016).

[7] Ottaviano, A., Li, G. Z., Huerta, C. E., Thuppul, A., Chen, Z., Dodson, C. A., & Wirz, R. E.: Plasma-material interactions for electric propulsion: challenges, approaches and future. In The 36th International Electric Propulsion Conference, Austria (2019).

[8] Wirz, R. E., Anderson, J. R., Goebel, D. M., & Katz, I.: Decel grid effects on ion thruster grid erosion. IEEE Transactions on Plasma Science **36** 2122-2129 (2008).

[9] Raitses, Y., Smirnov, A., Staack, D., & Fisch, N. J.: Measurements of secondary electron emission effects in the Hall thruster discharge. Physics of Plasmas **13** 014502 (2006).

[10] Stangeby, P. C.: The plasma boundary of magnetic fusion devices (Vol. **224**). Philadelphia, Pennsylvania: Institute of Physics Pub (2000).

[11] Fundamenski, W., Stangeby, P. C., & Elder, J. D.: A CFD onion-skin model for the interpretation of edge experiments. Journal of nuclear materials **266** 1045-1050 (1999).

[12] Bohm, D.: The characteristics of electrical discharges in magnetic fields. Qualitative Description of the Arc Plasma in a Magnetic Field (1949).

[13] Riemann, K. U.: Theory of the collisional presheath in an oblique magnetic field. Physics of plasmas **1** 552-558 (1994).

[14] 7 Riemann, K. U.: The influence of collisions on the plasma sheath transition. Physics of plasmas, **4** 4158-4166 (1997).

[15] Chodura, R.: Plasma–wall transition in an oblique magnetic field. The Physics of Fluids, **25** 1628-1633 (1982).

[16] Stangeby, P. C.: The Bohm–Chodura plasma sheath criterion. Physics of plasmas **2** 702-706 (1995).

[17] Franklin, R. N.:The active magnetized plasma-sheath over a wide range of collisionality. Journal of Physics D: Applied Physics **38** 3412 (2005).

[18] Ou, J., & Yang, J.: Properties of a warm plasma collisional sheath in an oblique magnetic field. Physics of Plasmas, **19** 113504 (2012).

[19] H.K. Malik, U. Stroth.: Nonlinear solitary waves (solitons) in inhomogeneous magnetized warm plasma with negative ions and nonisothermal electrons. Plasma Sources Sci. Technol. **17** 035005 (2008).

[20] Ghomi, H., & Khoramabadi, M.: Influence of ion temperature on plasma sheath transition. Journal of plasma physics, **76** 247-255 (2010).

[21] Emmert, G. A., Wieland, R. M., Mense, A. T., & Davidson, J. N.: Electric sheath and presheath in a collisionless, finite ion temperature plasma. The Physics of Fluids, **23** 803-812 (1980).

[22] Lafleur, Trevor, Pascal Chabert, and Jean-Paul Booth.: Secondary electron induced asymmetry in capacitively coupled plasmas. Journal of Physics D: Applied Physics **46** 135201 (2013).

[23] Raitses, Yevgeny, et al.: Effect of Secondary Electron Emission on Electron Cross-Field Current in $ E\times B $ Discharges. IEEE Transactions on Plasma Science **39** 995-1006 (2011).

[24] Nakamura, Keiji, Mitsuaki Tanaka, and Hideo Sugai. Energy measurements of sheath-accelerated secondary electrons in plasma immersion ion implantation. Surface and Coatings Technology **169** 57-60 (2003).

[25] Lafleur, Trevor, Pascal Chabert, and Jean-Paul Booth.: Secondary electron induced asymmetry in capacitively coupled plasmas. Journal of Physics D: Applied Physics **46** 135201 (2013).

[26] Ryutov, D. D.: Axial electron heat loss from mirror devices revisited. Fusion science and technology **47** 148-154 (2005).

[27] Sitnov, V. I., A. Ya Énder, and E. V. Yakovlev.: Current-voltage characteristics of underneutralized Knudsen thermionic converters with electron emission from the collector. Technical Physics **44** 373-380 (1999).

[28] Sheehan, J. P., et al.: A comparison of emissive probe techniques for electric potential measurements in a complex plasma. Physics of Plasmas **18** 073501 (2011).

[29] Modinos, A.: Theory of thermionic emission. Surface Science **115** 469-500 (1982).

[30] Campanell, M. D.: Possible mitigation of tokamak plasma–surface interactions using thermionic divertor plates with inverse sheaths. Physics of Plasmas **27** 042511 (2020).

[31] Ou, Jing, Xiaoyun Zhao, and Chunyun Gan.: Plasma-wall interaction in an electrostatic sheath of plasma containing a monoenergetic electron beam. Physics of Plasmas **23** 043510 (2016).

[32] Stangeby, P. C.: Plasma sheath transmission factors for tokamak edge plasmas.The Physics of fluids **27** 682-690 (1984).

[33] Taccogna, Francesco, Savino Longo, and Mario Capitelli.: Plasma-surface interaction model with secondary electron emission effects. Physics of Plasmas **11** 1220-1228 (2004).

[34] Malik HK, Jha YP and Kumar M.: Effect of collisions, ionization and non-extensivity on sheath formation in an electronegative warm plasma under electron emission from the wall. Journal of Theoretical and Applied Physics. 2022 Nov 29.

[35] Sizonenko, V. L.: The effect of high secondary-electron emission on plasma-layer. ZHURNAL TEKHNICHESKOI FIZIKI **51** 2283-2291 (1981).

[36] Amemiya, H., B. M. Annaratone, and J. E. Allen.: The double sheath associated with electron emission into a plasma containing negative ions. Journal of plasma physics **60** 81-93 (1998).

[37] Schwager, L. A.: Effects of secondary and thermionic electron emission on the collector and source sheaths of a finite ion temperature plasma using kinetic theory and numerical simulation Physics of Fluids B: Plasma Physics **5** 631-645 (1993).

[38] Jha, Yetendra Prasad, et al.: Electronegative warm plasma and material interaction under secondary electron emission. *Materials Today: Proceedings* (2022).

[39] Ordonez, C. A.: Fully kinetic plasma-sheath theory for a cold-electron emitting surface. Physics of Fluids B: Plasma Physics **4** 778-783 (1992).

[40] Franklin, R. N., and J. Snell.: The Boltzmann relation in electronegative plasmas: When is it permissible to use it? Journal of Plasma Physics **64** 131-153 ((2000)).

[41] Ghim, Young-chul, and Noah Hershkowitz.: Experimental verification of Boltzmann equilibrium for negative ions in weakly collisional electronegative plasmas. Applied Physics Letters **94** 151503 (2009).

[42] Lyra, M. L., and C. Tsallis.: Nonextensivity and multifractality in low-dimensional dissipative systems. Physical review letters **80** 53 ((1998)).

[43] Araghi, F., & Dorranian, D.: Effect of negative ions on the characteristics of plasma in a cylindrical discharge. Journal of Theoretical and Applied Physics **7** 1-8 (2013).

[44] Dorranian, D., & Alizadeh, M.: Effect of negative oxygen ions on the characteristics of plasma in a cylindrical DC discharge. Journal of Theoretical and Applied Physics: **8** 1-6 (2014).

[45] Malik, L., Rawat, S., Kumar, M. and Tevatia, A.: Simulation studies on aerodynamic features of Eurofighter Typhoon and Dassault Rafale combat aircraft. Materials Today: Proceedings, **38**, pp.191-197 (2021).

[46] Malik, L., Escarguel, A., Kumar, M., Tevatia, A. and Sirohi, R.S.: Uncovering the remarkable contribution of lasers peak intensity region in holography. Laser Physics Letters, **18**, p.086003 (2021).

[47] Malik, L. and Tevatia, A.: Comparative Analysis of Aerodynamic Characteristics of F16 and F22 Combat Aircraft using Computational Fluid Dynamics. Defence Science Journal, **71** *(*2021.).

[48] Malik, L., Kumar, M. and Singh, I.V.: A Three-Coil Setup for Controlled Divergence in Magnetic Nozzle. IEEE Transactions on Plasma Science, **49**, pp.2227-2237 (2021).

[49] Safa, N. N., Ghomi, H., & Niknam, A. R.: Effect of the q-nonextensive electron velocity distribution on a magnetized plasma sheath. Physics of Plasmas **21** 082111 (2014).

[50] Asserghine, A., El Kaouini, M., & Chatei, H.: Investigation of magnetized plasma sheath in the presence of q-nonextensive electrons and negative ions. Materials Today: Proceedings **24** 24-28 (2020).

[51] Chen, F. F.: Introduction to Controlled Fusion. In Introduction to Plasma Physics (pp. 279-318). Springer, Boston, MA (1974).

[52] Borgohain, D. R., & Saharia, K.: Behavior of collisional sheath in electronegative plasma with q-nonextensive electron distribution. Physics of Plasmas **25** 032122 (2018).